Environmental Nanotechnology, Monitoring & Management 1–2 (2014) 14–23

Contents lists available at ScienceDirect

Environmental Nanotechnology, Monitoring & Management

journal homepage: www.elsevier.com/locate/enmm

Treatment of olive mill based wastewater by means of magnetic nanoparticles: Decolourization, dephenolization and COD removal

Nashaat N. Nassar[a,b,*], Laith A. Arar[b], Nedal N. Marei[a,b], Mahmoud M. Abu Ghanim[b], Marwan S. Dwekat[b], Shadi H. Sawalha[b]

[a] Department of Chemical and Petroleum Engineering, University of Calgary, 2500 University Drive NW, Calgary, Alberta, Canada
[b] Department of Chemical Engineering, An-Najah National University, P.O. Box 7, Nablus, Palestine

ARTICLE INFO

Article history:
Received 3 July 2014
Received in revised form 2 September 2014
Accepted 4 September 2014

Keywords:
Adsorption
Olive mill wastewater
Iron oxide
Decolourization
Fixed bed
Nanoparticle

ABSTRACT

Olive mill wastewater (OMW) is an environmental concern that has been highlighted as a serious environmental problem in the Mediterranean basin countries because of its high organic load and phytotoxic and antibacterial phenolic compounds, which resist biological degradation. Consequently, this type of wastewater represents a huge challenge for the conventional wastewater treatment techniques as it can impact the lifetime of bacteria needed for the treatment. Iron-oxide nanoparticles are attractive for wastewater treatment for two important reasons. First, nanoparticles can remove pollutants from wastewater rapidly. Second, this magnetic type of nanoparticles could be separated easily using a magnet after finishing treatment process. In this study, we aimed at investigating the effectiveness of the magnetic iron oxide nanoparticles in the removal of large organic contaminants from OMW. Batch and continuous mode processes were applied on OMW treatment to determine the effect of contact time, solution pH, coexisting contaminants and the adsorption isotherm.

The results showed that the adsorption was fast and the adsorption reached equilibrium within less than 30 min. The adsorption equilibrium data fit very well to the Brunauer–Emmett–Teller (BET) Model, indicating multi-layers adsorption. The adsorption of major pollutants was associated to an efficient removal of coexisting contaminants such as heavy metals and free ions. The adsorption of OMW pollutants was dependent on pH of the solution. Finally, continuous-mode process was tested successfully using a packed bed column that combined sand filtration with magnetic nanoparticles to decolourize OMW effluent. This study will provide valuable insight on the effect of nanoparticles toward the treatment and recyclability of olive mill wastewater, which is crucial for the local olive mill industry. After seeing the successful achievement of integrating nanoparticles with fixed bed filtration, a preliminary process description and cost estimation of stand-alone plant (with a capacity of 4 m^3/h) for OMW treatment were considered in this study. Process capital and annual operating costs were estimated to be $12,306 and $476/year, respectively.

1. Introduction

Olive mill wastewater (OMW) is generated by the olive oil mills during the extraction of olive oil (Ben Sassi et al., 2008; Eroğlu et al., 2008; Jarboui et al., 2008; Hanafi et al., 2009; Hanifi and El Hadrami, 2009; Ipsilantis et al., 2009; Kallel et al., 2009; Choy et al., 2005). Around 6×10^6 m^3 of OMW is produced yearly worldwide, of which 98% is produced in the Mediterranean basin (Zorpas and Costa, 2010). These types of effluents are produced seasonally during September to November of every year in the Mediterranean region, where there is a major production of olive oil. It is anticipated that for every ton of olive fruits processed approximately 1.2–1.8 m^3 of wastewater is generated, by three-phase olive mills (centrifugal systems) (Nassar, 2007). Actually, OMW resulting from the production processes in the Mediterranean basin surpasses 30 MCM per year (El-Gohary et al., 2009). OMW contains appreciable amount of organic materials with a high amount of toxicity/phytotoxicity-associated compounds, which

* Corresponding author at: Department of Chemical and Petroleum Engineering, University of Calgary, 2500 University Drive NW, Calgary, Alberta, Canada. Tel.: +1 403 2109770.
E-mail address: nassar@ucalgary.ca (N.N. Nassar).

http://dx.doi.org/10.1016/j.enmm.2014.09.001

resist biological degradation (Coskun et al., 2010). Typically, due to the current absence of appropriate treating technologies for OMW effluents, OMW is discharged directly into sewer systems, valleys, and uncontrolled ponds, despite the fact that such discarding methods are forbidden in many Mediterranean countries (Shaheen and Karim, 2007; Brunetti et al., 2007; Boukhoubza et al., 2008; Dhaouadi and Marrot, 2008; Jarboui et al., 2008; Hanifi and El Hadrami, 2009). The inadequate and uncontrolled disposal methods of OMW to the water bodies possess an environmental concern as these effluents contain appreciable amount of COD and BOD concentrations, high amount of microbial growth-inhibiting compounds, such as phenolic compounds and tannins (Hanifi and El Hadrami, 2009; Kallel et al., 2009; Lucas and Peres, 2009). Nonetheless, a number of physical, chemical and biological treatment methods have been reported in literature; including flotation and sedimentation (Achak et al., 2008), sand filtration (Achak et al., 2009a,b), ozonation (Chedeville et al., 2009), membrane filtration (Paraskeva et al., 2007; Dhaouadi and Marrot, 2008; Akdemir and Ozer, 2009), neutralization with addition of acid, advanced chemical oxidation (Fenton reaction) (Gomec et al., 2007; Zorpas and Costa, 2010), adsorption by activated carbon and aerobic and anaerobic digestions (Azbar et al., 2008a,b; Boubaker and Ridha, 2008). These methods, however, are limited because they are too expensive to find a wide application, ineffective in meeting stringent effluent standards, and could result in huge amount of sludge. Nanoparticle technology (i.e., the technology related to the preparation and application of materials at nanoscale, 1–100 nm) has emerged as a fascinating area of interest for removal of various contaminants from wastewater effluents (Nassar, 2012a, 2013; Savage and Diallo, 2005; El Saliby et al., 2009; Kaur and Gupta, 2009; Narayan, 2010; Xu et al., 2012). Nanoparticles can be employed as an alternate method for OMW treatment. Because of their relatively low cost and unique properties such as large surface area, high reactivity, high specificity, self-assembly and dispersibility nanoparticles have promising perspectives for OMW treatment. With a particular affinity toward organic compounds, these nanoparticles are also magnetic, allowing for their magnetic separation and removal from the process stream. Because these particles could be prepared and applied in situ, the materials costs are reduced. Several researchers have reported about the employment of iron-based nanoadsorbents in removing various pollutants from wastewater (Nassar, 2010a,b, 2012a,b; Tratnyek and Johnson, 2006). The utilization of photocatalysis approach with different nanoparticles for OMW treatment has been successfully reported (Ruzmanova et al., 2013; Ochando-Pulido et al., 2013). However, to the best of our knowledge, there have been no reports on the application of magnetic assisted-nanoparticle adsorption technology on the removal of contaminants from olive mill wastewater.

This study is aimed at investigating the effectiveness of the magnetic iron oxide nanoparticles for the adsorptive removal of large organic contaminants from OMW effluent. In this study, a batch-contact-time method is used for the treatment of real OMW samples obtained from selected local olive mill factories in the West Bank, Palestine. The following operating and experimental parameters are investigated to find out the optimum conditions for enhancing the treatment efficiency, namely: contact time, adsorption isotherm, coexisting pollutants and solution pH. Further, a continuous-mode process using a fixed bed column that combines sand filtration with magnetic nanoparticles to decolourize OMW effluent has been tested. In addition, a preliminary process design and cost estimation of stand-alone OMW treatment plant was reported. This study provides valuable insight on the effect of nanoparticles toward the treatment and recyclability of olive mill wastewater, which is crucial for the local olive mill industry.

Table 1
Characteristics of different fresh OMW samples collected from different olive mill presses in Palestine.

	Nablus	Qalqilia	Jenin
COD (mg/L)	153×10^3	136×10^3	10×10^3
pH	5.04	4.41	4.49

2. Materials and methods

2.1. Adsorbent

Magnetic nanoparticles (γ-Fe_2O_3) purchased from Alfa Aesar (Ontario, Canada) were used as an adsorbent. Its measured particle size and surface area were 10 ± 2.0 nm and 93 m^2/g, respectively. The nanoadsorbents were used as received without further purification. Structure and particle size were determined using X-ray Ultima III Multi Purpose Diffraction System (Rigaku Corp., The Woodlands, TX) with Cu Kα radiation operating at 40 kV and 44 mA with a θ–2θ goniometer. Surface area of the nanoparticles was measured by a surface area and porosity analyzer (TriStar II 3020, Micromeritics Corporate, Norcross, GA) by performing N_2-physisorption at 77 K. The sample was degassed at 150 °C under N_2 flow overnight before analysis. Surface area was calculated using Brunauer–Emmett–Teller (BET) equation. External surface area was obtained by *t*-plot method, and there was no significant difference between the surface areas obtained by BET and *t*-plot methods, indicating that the selected nanoparticles have no significant porosity and maintain a high external surface area.

2.2. Adsorbate

Three olive mill wastewater samples were obtained from the main drainpipe of three different olive mill presses located at different cities in Palestine, namely: Nablus, Qalqilia and Jenin. The three samples were obtained in November 1, 2013 from a two-phase full automatic presses. The samples were collected in pre-washed dried tightly capped glass vials and kept stored in a dark incubator at 21 °C prior to analysis, which was performed immediately after stabilization. These samples were analyzed prior to treatment for pH and chemical oxygen demand (COD); the results of analysis are shown in Table 1. As seen, in all cases, OMW is slightly acidic, pH < 7.0. Nablus sample showed the highest COD concentration probably due to different types of environmental conditions available for the olive trees there. Accordingly, the Nablus sample was considered in this study and was further analyzed prior to treatment for electrical conductivity (EC), biological oxygen demand (BOD), total suspended solids (SS), total dissolved solids (TDS), and density; the results of analysis are presented in Table 2. It is worth noting here that these values are in good agreement with those reported in literature (Zorpas and Costa, 2010).

Table 2
Main characteristics of fresh OMW sample obtained from olive mill press in the city of Nablus, before and after sedimentation.

Parameter	Before sedimentation	After sedimentation (supernatant)
COD (mg/L)	153×10^3	89×10^3
BOD_5 (mg/L)	71.4×10^3	52.8×10^3
TOC (mg/L)	57.5×10^3	33.5×10^3
TSS (mg/L)	51×10^3	1.3×10^3
TDS (mg/L)	57.2×10^3	35×10^3
EC (mS/cm)	8.29	9.22
Density (kg/m^3)	974	961
pH	5.04	5.0

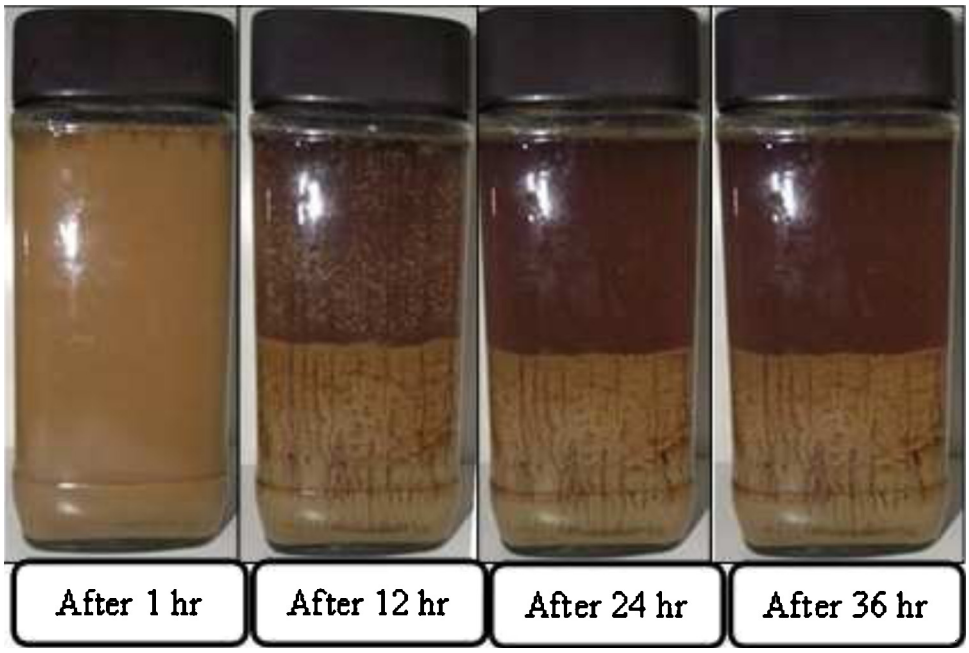

Fig. 1. Photographs taken at different times for a selected OMW sample for a period of 36 h.

2.3. Chemicals

A 70% (w/w) nitric acid (HNO_3) and 99% (w/w) sodium hydroxide (NaOH) purchased from Riedel de Haen (Germany) were used at concentration of 0.5 M for pH adjustment. For heavy metals determination tests, a standard solution containing $CrCl_2{\cdot}6H_2O$, $Cu(NO_3)_2{\cdot}5H_2O$ and $FeCl_3$ obtained from Riedel de Haen (Germany) were used as sources for Cr^{+2}, Cu^{+2} and Fe^{+3}, respectively. A KHP purchased from Sigma Aldrich (Germany), was used to prepare a COD calibration curve. 97% (w/w) ethyl acetate and methanol and 70% (w/w) HCl purchased from Frutarom (Israel), 99% (w/w) sodium sulphate and 97% 3,4 dihydroxy benzoic acid purchased from Sigma Aldrich (Germany) were used for polyphenols determination test. A 99% KOH purchased from Sigma Aldrich (Germany) was used for BOD_5 test. A 91% (w/w) phenol purchased from Riedel de Haen (Germany) was used as a model molecule to mimic OMW sample.

2.4. Stabilization of OMW sample

Before conducting any adsorption experiment, the fresh OMW sample was monitored for 36 h to allow for the big suspended particles to precipitate. Fig. 1 shows photographs of OMW sample taken at different time intervals. As seen, the fresh OMW sample was initially completely turbid and homogeneous. After 12 h it starts to separate into two phases, at the macro level, the upper layer, which is mainly the supernatant, and the lower layer, which contains sludge, dirt and suspended solids. After 24 h, the sample was completely stable and separated into two clear layers, at the macro level. Then, the two layers were remained unchanged. Hence, the sedimentation time needed is concluded to be 24 h to obtain a very clear supernatant. Worth noting here that a very thin layer of oily phase was appeared on the top of the supernatant, which was skimmed off before taking the supernatant for analysis or adsorption test. After that the supernatant was decanted and transferred for further analysis and adsorption tests. Table 2 shows the characteristics of the supernatant. As seen, the sample characteristics have changed after precipitation. COD value was still very high though. The reduction in the COD value by sedimentation was approximately 40%. Also, the reduction in the BOD_5 value was approximately 21%. Again, the pH of the supernatant was still slightly acidic which could be due to the presence of high concentration of phenolic compounds and carboxylic acids, which are categorized as weak acids.

2.5. Batch adsorption experiments

Phenolic compounds (i.e., phenol and polyphenols) are believed to be the coloring agent of OMW since it recorded to be the major pollutants (Ugurlu and Kula, 2007). Accordingly, to understand the adsorption mechanism of OMW pollutants, phenol was chosen as a model molecule. Therefore, in addition to the real OMW sample, synthetic wastewater samples containing different known initial concentrations of phenol were prepared for the adsorption test as well. Batch-mode adsorption method was employed in this study by exposing a specified dried mass of γ-Fe_2O_3 nanoparticles to an aqueous solution containing a specified initial concentration of contaminants. Then, the mixture was shaken for a certain time at 298 K. For kinetics study, time-dependent adsorption process was conducted by exposing a certain amount of nanoparticles to a solution containing a specified concentration of pollutant for fixed preselected time intervals. In this study, for phenol, 0.05 g of γ-Fe_2O_3 nanoparticles were added to 5 mL aqueous solution containing a 100 ppm concentration of phenol at 298 K and a pH of 7.5. The mixture was shaken for 180 min, unless otherwise noted. To determine the adsorption equilibrium time required for saturation, samples were selected at different times during the 180 min and analyzed for phenol concentration. In a similar manner, for real OMW sample, 0.1 g of γ-Fe_2O_3 nanoparticles were added to a 5 mL solution at a specified COD, 298 K and a pH equal 5. The mixture was shaken for 90 min, unless otherwise noted. For pH-dependent studies, OMW model pollutant (phenol) and real OMW adsorption pH experiments were conducted at 298 K for a mixing time of 24 h and a pH range of 2–12. To adjust the solution pH, HNO_3 or NaOH were used. For isotherm experiments, 0.05 g of γ-Fe_2O_3 nanoparticles were added to a set of 5 mL vials containing different initial concentration of phenol ranged from 0 to 400 ppm at a pH equal to 7.5 and at temperature of 298 K. The mixture was left shaking for 24 h. In a similar manner, for OMW sample, 0.1 g of γ-Fe_2O_3 nanoparticles

were added to a set of 5 mL test tubes containing different COD concentrations ranged from 100 to 3200 times dilution at pH 5 and temperature of 298 K. The mixture was left shaking for 24 h. For the effect of coexisting contaminants study, the following ions were measured before and after adsorption for a selected OMW sample using atomic absorption (AA) (iCE 3400, Thermo Fisher Scientific, USA) and flame photometer (PFP7, Jenway, UK): Cu^{+2}, Cr^{+2}, Fe^{+2}, Na^{+}, Ca^{+2}, and K^{+}. A calibration curve was constructed between 0 and 20 ppm, by using prescribed standard solutions.

In all experiments, the γ-Fe_2O_3 nanoparticles containing adsorbed contaminants were separated from the mixture by a magnet and the supernatant was decanted. The initial and residual concentration of phenol in the solution was measured by UV-vis spectrophotometry (UV-VIS-NIR-3101PC, Shimadzu). Concentration of phenol was measured at the specified wavelength (λ_{max} = 254 nm). A calibration curve of UV–vis absorbance at same wavelengths against the phenol concentration was established, using prepared standard model solutions with known concentrations. UV–vis spectra of phenol in solution were selected on the basis of the absorption linearity range. For the case of OMW, the initial and residual concentration of contaminants in OMW sample was measured by the chemical oxygen demand (COD) test using (Digital Reactor Block DRB 2000, HACH, Germany) and following a standard procedure (ASTM, 1995). The adsorbed amount of contaminants per mass of nanoparticles (mg/g) was determined by the mass balance in Eq. (1):

$$Q = \frac{C_o - C}{m} V \tag{1}$$

where C_o is the initial concentration of phenol or COD in the solution (mg/L), C is the final concentration of phenol or COD in the supernatant (mg/L), V is the solution volume (L), and m is the dry mass of γ-Fe_2O_3 nanoparticles (g). For equilibrium data, C_e replaces C, and Q_e replaces Q in Eq. (1).

2.6. Continuous adsorption experiment

Continuous-mode decolourization of OMW was achieved by using a fixed-bed column made of glass tube of 50 cm height and 1 cm inner diameter. At the bottom of the column, a plastic sieve was attached followed by a layer of cotton and 2 cm layer sand to prevent nanoparticles from escaping out of the column. Approximately 10 g of virgin fine locally supplied sand particles mixed well with different mass% of γ-Fe_2O_3 nanoparticles were packed in the column to yield the desired bed height (~30 cm). 5 and 10 wt% of nanoparticles were considered in this study. The column was then filled up with another 2 cm layer of sand particles in order to provide a uniform flow of the solution through the column. OMW solution of 79,000 mg/L COD concentration at temperature of 298 K and pH 5 was driven by gravity downward through the column at a desired flow rate of 0.03 L/h by maintaining a constant level of OMW solution in the column. The OMW solutions at the outlet of the column were collected at different time intervals and the color change was noted and the concentration was measured. In this set of experiments, the time zero was considered after the first drop of water comes out from the fixed-bed column.

One sample was selected from the breakthrough curve for polyphenols removal test, whereby 1 mL of the sample was diluted into 100 mL distilled water. The sample was acidified up to pH = 2 with HCl and then followed by extraction with 20 mL ethyl acetate at 298 K for three times. The sample was dried by contacting with 2 g sodium sulphate crystals for 30–40 min. The ethyl acetate left in the extraction was vaporized using a rotary evaporator and the residual solution was mixed with 50 mL of a mixture of water/methanol at 40/60 volumetric ratio (Garcia et al., 2000). The final solution was a liquid that contains all the phenolic compounds of the sample. For measuring total polyphenol, the sample extracted by ethyl acetate was measured by a spectrophotometer at 725 nm and using a standard curve of 3,4 dihydroxy benzoic acid, where total polyphenol could be determined (Box, 1983).

3. Modeling

Adsorption kinetics of contaminants onto nanoparticles surface were modeled using the Lagergren pseudo first-order and pseudo-second-order models. The adsorption isotherms were modeled using the Brunauer–Emmett–Teller (BET) adsorption models.

3.1. Adsorption kinetics

Modeling of the adsorption kinetics of the batch experiments was achieved using the Lagergren pseudo first-order model in Eq. (2) (Ho, 2004) and pseudo-second-order model in Eq. (3) (Ho and McKay, 1998).

$$\frac{dQ_t}{dt} = k_1(Q_e - Q_t) \tag{2}$$

$$\frac{dQ_t}{dt} = k_2(Q_e - Q_t)^2 \tag{3}$$

where Q_e and Q_t are the amount of pollutants adsorbed onto the nanoparticles (mg/g) at equilibrium and at any time, t (min), respectively, and K_1 (min^{-1}) and K_2 (g/mg min) are the equilibrium rate constants of first order and second order adsorption, respectively. Nonlinear Chi-square analysis were conducted for comparing the best-fit-model by Eq. (4) (Montgomery and Runger, 2006):

$$\chi^2 = \sum \frac{(Q_e - Q_{emodel})^2}{Q_{emodel}} \tag{4}$$

where Q_e and Q_{emodel} are the adsorbed amount of contaminants obtained experimentally and by model fitting, respectively. The lower the value of χ^2 the better the fitting.

3.2. Brunauer–Emmett–Teller adsorption model (BET)

The BET model has been widely used to correlate adsorption isotherm experimental data (Teller et al., 1938). This model describes the multilayer adsorption phenomena for gas–solid equilibrium systems and liquid–solid systems (Ebadi et al., 2009; Wang et al., 1998). The BET model can be expressed as follows:

$$Q = Q_{max} \frac{K_S C_e}{(1 - K_L C_e)(1 - K_L C_e + K_S C_e)} \tag{5}$$

where Q is the amount of pollutants (mg/g) adsorbed at equilibrium; Q_{max} the maximum adsorption capacity (mg/g); C_e the equilibrium concentration of pollutants in the aqueous phase (mg/L); and K_S (L/mg) and K_L (L/mg) are the equilibrium constants of adsorption for the first and the upper layers, respectively. Again, χ^2 analysis (Eq. (4)) was also employed for finding the goodness of fittings.

4. Results and discussion

4.1. Effect of contact time (adsorption kinetics)

Time-dependent experiments were conducted at 298 K to determine the pollutant adsorptive removal rate by the nanoparticles. The initial phenol concentration was 100 ppm and two different initial COD concentrations were considered for the case of real OMW samples, namely 962 and 460 mg/L. Panels a and b of Fig. 2 show the change in the amount adsorbed of phenol and pollutants from synthetic and real OMW, respectively, as a function of contact time together with kinetic model fit. As seen, in all cases, adsorption was

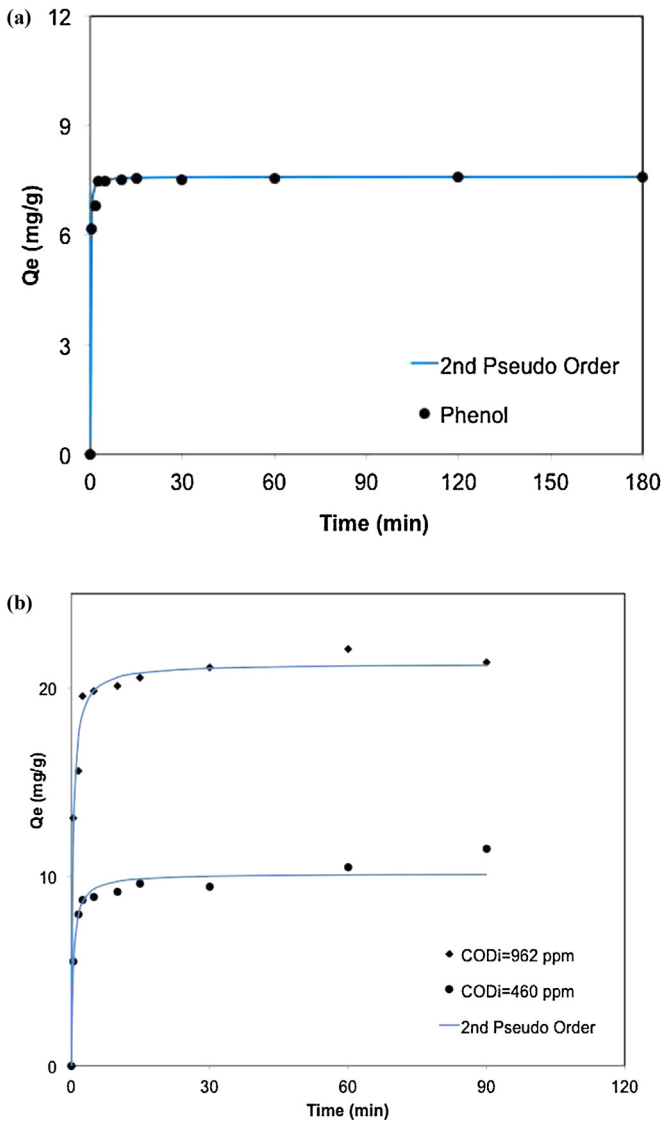

Fig. 2. Effect of contact time on the adsorptive removal of (a) phenol at initial concentration of 100 ppm and pH = 7.5 and (b) OMW pollutants at initial COD of 962 and 460 mg/L at pH = 5. Points are experiments; lines are second-pseudo-order model (Eq. (3)). Other experimental conditions are T = 298 K, shaking rate = 300 rpm.

quite fast, as adsorption equilibrium was reached within 10 min for phenol and less than 30 min for real OMW. This is not surprising as the selected nanoparticles are nonporous. Therefore, one would anticipate that external adsorption is dominant and no intraparticle diffusion is available to retard the adsorption rate (Nassar, 2010a; Nassar and Ringsred, 2012). Unlike the classical adsorbents such as activated carbon and activated alumina, where adsorption equilibrium time could take days (Crittenden, 2005). To further investigate the kinetic mechanism that controls the adsorption process, the experimental data were fitted to the Lagergren pseudo-first-order model (Ho, 2004) and pseudo-second-order model (Ho and McKay, 1998) presented previously in Eqs. (2) and (3); respectively.

Table 4
Estimated values of the kinetic parameters of the pseudo-first-order and pseudo-second-order models for the adsorptive removal of OMW pollutants by γ-Fe_2O_3 nanoparticles at different initial concentrations. Other experimental parameters are T = 298 K, pH = 5, shaking rate = 300 rpm.

COD_i (mg O_2/L)	962	460
$Q_{e,exp}$ (mg/g)	23.03	10.2
Pseudo-first-order		
Q_e (mg/g)	18.75	8.72
K_1 (min^{-1})	85.15	220.07
χ^2	4.497	3.09
Pseudo-second-order		
Q_e (mg/g)	21.3	10.2
K_2 (g/mg min)	0.133	0.227
χ^2	0.295	0.262

Tables 3 and 4 show the estimated kinetic parameters pertaining to the two models. As shown in panels a and b of Fig. 2, and on the basis of Chi values presented in Tables 3 and 4, both models fit well to the experimental data with the pseudo-second-order model being the best fit for the two cases, synthetic and real OMW samples. This suggests that, owing to good degree of mixing and extent dispersion of nanoparticles, adsorption is only affected by two mechanisms; first, rapid adsorption due to electrostatic attraction followed by slow gradual adsorption of pollutants onto nanoparticle surface by complexation (Nassar and Ringsred, 2012; Franco et al., 2014a; Nassar, 2012a). It is worth noting here that the estimated theoretical values of Q_e (i.e., by the kinetic model) were in excellent agreement with the ones obtained experimentally, as seen in Tables 3 and 4.

4.2. Effect of solution pH

Experiments were performed to find the optimum pH on the adsorption of phenol and OMW pollutants onto γ-Fe_2O_3 nanoparticles using different initial pH values changing from 2.5 to 12 and temperature of 298 K. Panels a and b of Fig. 3 show the change in the amount adsorbed of phenol and pollutants from synthetic and real OMW wastewater, respectively, as a function of solution pH. As shown in panel a, for phenol, it can be clearly seen that the removal of phenol from wastewater is pH independent. This is not surprising as the point of zero charge (pH_{pzc}) of iron oxide particle is around 7.5 (Balistrieri and Murray, 1981; Nassar and Ringsred, 2012). Therefore, at a pH higher than pH_{pzc}, the nanoparticle surface is negatively charged attracting cations, whereas at a lower pH, the surface is positively charged attracting anions. Phenol is a water-soluble weak acid. In aqueous solution, the phenol molecule dissociates negative anion as illustrated in reaction (R1). As per (R1), hydrogen atom leaves the molecule to form H_3O^+ and resulted in a negatively charged phenoxide ion. Hence, at low pH value, acidic media, an electrostatic attraction exists between the positively charged surface of the nanoparticles and the phenoxide molecules (Clifford and Luis, 1979).

$$C_6H_5OH + H_2O \Leftrightarrow C_6H_5O^- + H_3O^+ \quad \text{(R1)}$$

On the other hand, in an alkaline environment, at high values of pH, phenol reacts with NaOH as per reaction (R2) to form a

Table 3
Estimated values of the kinetic parameters of the pseudo-first-order and pseudo-second-order models for the adsorptive removal of phenol by γ-Fe_2O_3 nanoparticles. Experimental parameters are T = 298 K, pH = 7.5, shaking rate = 300 rpm and C_o = 100 ppm.

$Q_{e,exp}$ (mg/g)	Pseudo-first-order			Pseudo-second-order		
	Q_e (mg/g)	K_1 (min^{-1})	χ^2	Q_e (mg/g)	K_2 (g/mg min)	χ^2
7.6000	7.604	1.602	0.0043	7.598	2.333	0.0013

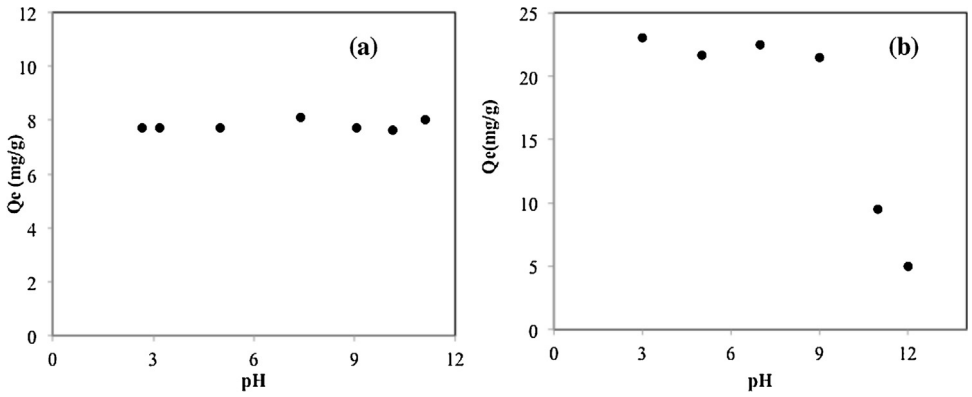

Fig. 3. Effect of pH on the adsorptive removal of (a) phenol from wastewater by γ-Fe_2O_3 nanoparticles at initial concentration of 100 ppm and nanoparticle dose = 0.1 g per 10 mL, (b) OMW pollutants by γ-Fe_2O_3 nanoparticles at initial concentration COD_i = 978 mg/L and nanoparticle dose = 0.1 g per 10 mL. Other experimental conditions are T = 298 K, mixing time = 24 h.

Table 5
Estimated parameters for BET model at temperature 298 K.

	pH	K_l (L/mg)	K_s (L/mg)	Q_{max} (mg/g)	χ^2
OMW	5	1.4×10^{-3}	1.8×10^{-4}	69.6	1.025
Phenol	7.5	6.0×10^{-3}	2.7×10^{-3}	79.09	0.240

positively charged sodium phenoxide, which prefers adsorption onto a negatively charged surface (Clifford and Luis, 1979).

$$C_6H_5OH + NaOH \Leftrightarrow C_6H_5ONa^+ + H_2O \quad (R2)$$

For the case of real OMW, as shown in panel b of Fig. 3, the amount adsorbed was independent of pH in region of 3–9. In fact, this result is expected and not far away from the results of model molecule, phenol. This indicates that OMW, which contains plenty of pollutants, has a considerable extent of phenol and polyphenol compounds. However, adsorption decreased sharply with further increase in solution pH. This could be probably due to the increase of solubility of the pollutant at high pH values.

4.3. Adsorption isotherms

To assess the efficiency of γ-Fe_2O_3 nanoparticles in removing phenol and pollutants from OMW samples, isotherm studies were conducted at different solution pH and a temperature of 298 K. Panels a and b of Fig. 4 show the phenol and OMW adsorption isotherms, respectively, together with the BET model fitting. As shown in Fig. 4, in both cases, the amount adsorbed increased exponentially with the equilibrium concentration, and the adsorption isotherms exhibited Type III behavior according to the IUPAC (Sing et al., 1982). These types of isotherms are characteristic of multilayer adsorption on non-porous solids with weak adsorbent-adsorbate interactions (Franco et al., 2014b). Adsorption proceeds as the interaction between an adsorbate and an adsorbed layer is greater than the interaction with the adsorbent surface where adsorption increases exponentially; this process leads to the formation of multilayers of pollutant on the nanoparticle surface, mainly at high initial concentrations (Franco et al., 2014b). This also confirms the results of the kinetic study, where fast adsorption equilibrium was achieved due to non-porous structure. Accordingly, the BET model was used to describe the experimental data of adsorption isotherms. The estimated model parameters are listed in Table 5. As seen in Table 5, according to the χ^2 values, the BET showed a good fit to the experimental data, which confirms the multilayer adsorption mechanism. These results are in good agreement with those reported by Franco et al. (Franco et al., 2014a,b) who reported the adsorptive removal of oil from fresh water and

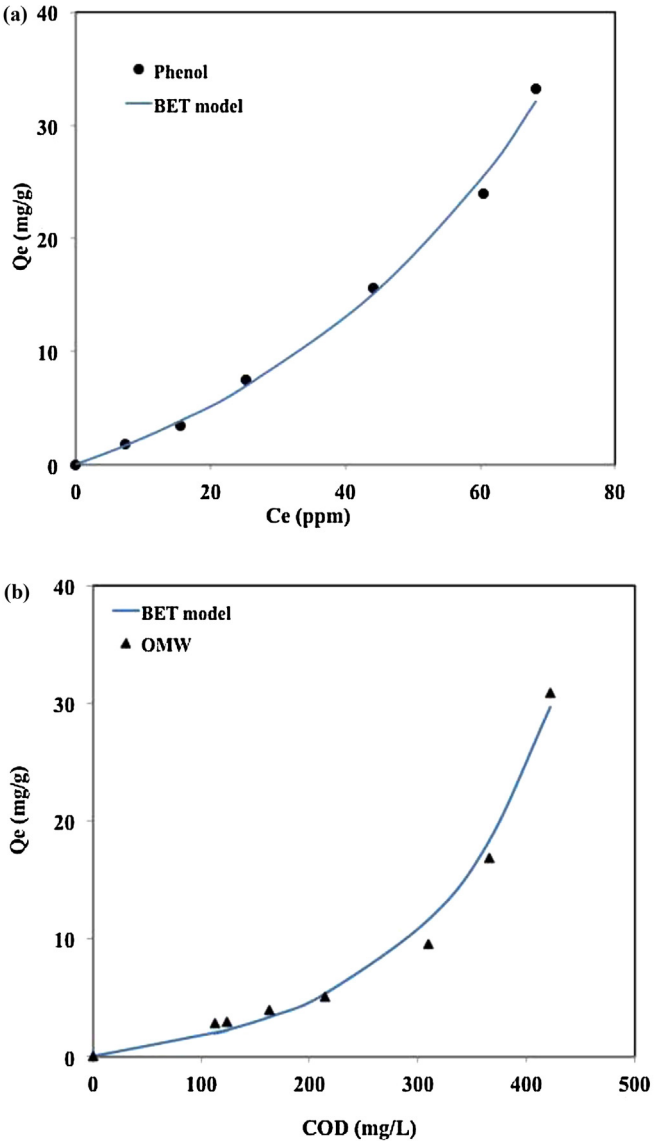

Fig. 4. Adsorption isotherm of (a) phenol at pH = 7.5 and (b) OMW at pH = 5 by γ-Fe_2O_3 nanoparticles. Points are experimental data and solid lines are from the BET model (Eq. (5)). Other experimental conditions are: T = 298 K, mixing time = 24 h.

Table 6
Adsorption of coexisting ions in the supernatant of OMW sample onto γ-Fe_2O_3 nanoparticles. Adsorbent dose is 0.1 g per 10 mL sample, T = 298 K, pH = 5, mixing time = 24 h.

	Before adsorption	After adsorption	% Removal
Fe^{+3} (mg/L)	41.51	8.36	79.86
Cr^{+2} (mg/L)	4.89	1.37	71.98
Cu^{+2} (mg/L)	8.23	3.78	54.07
K^{+} (mg/L)	10,162	5120	49.62
Ca^{+2} (mg/L)	1520	850	44.08
Na^{+} (mg/L)	2213	805	63.62

salted-water emulsions by alumina nanoparticles functionalized with vacuum gas oil molecules, and Weng and Pan, who studied the adsorption of methylene blue onto bio-sludge ash (Weng and Pan, 2006) and spent activated clay (Weng and Pan, 2007) and by Wang et al. (1998) who studied the equilibrium constants for the first layer and subsequent adsorption of dye onto sludge particles.

4.4. Effect of coexisting pollutants

In addition to the organic pollutants, OMW contains appreciable amount of coexisting ions such as Fe^{3+}, Cr^{2+}, Cu^{2+}, Ca^{2+}, K^{+}, and Na^{+}. These ions can compete for the adsorption sites and interfere in the removal efficiency. As a result, the adsorption of these coexisting ions was studied at initial pH of 5.0 and 298 K by exposing 10 mL of fresh supernatant (after sedimentation, COD = 89×10^3 mg/L) of real OMW sample to 0.1 g of γ-Fe_2O_3 nanoparticles for 24 h. After that the sample was taken for elemental analysis. The results are shown in Table 6. As seen, in addition to their organic removal, nanoparticles were able to adsorb different ions. The competitive adsorption ability varies from one ion to another and is related to a number of factors, such as molecular mass, ion charges, hydrated ionic radius and hydration energy of the metals (Nassar, 2010b). This indicates that the nanoparticle surface is highly attractive to a large extent of OMW contaminants and multi adsorption would occur.

4.5. Fixed-bed analysis

In real application, most adsorbents are used in continuous flow configuration (e.g., fixed-bed adsorption) rather than the batch process. This study, however, deals with the application of nanoparticles for in situ remediation rather than fixed bed adsorption. Hence, the nanoparticles can be utilized in situ, within the contaminated zone, such as sedimentation tank, pond, lakes, etc. where treatment is needed. Nevertheless, combining the nanoparticle technology with the sand filtration process is tested in this study.

Fig. 5 shows the breakthrough curves obtained for OMW pollutant adsorption in a fixed bed process (sand + 5 and 10 wt% nanoparticles), at a constant flow rate of 0.03 L/h and COD inlet concentration of 79,000 mg/L. As expected, the presence of nanoparticles increased the breakthrough time, where OMW pollutants had more time to contact with sand and nanoparticles. This resulted in higher removal efficiency of OMW pollutants in the fixed bed column. Further, the presence of nanoparticles caused a significant decrease in the COD concentration of the effluent at the same time. Hence, high adsorption capacity could be observed in the fixed bed containing nanoparticles. This could be because of the increase in the surface area of adsorbent in the presence of nanoparticles, which provided more active sites for the adsorption.

Fig. 6 shows a photograph for a set of different samples obtained at different times from the fixed-bed column experiments in the presence of 10 wt% nanoparticles together with the control sample.

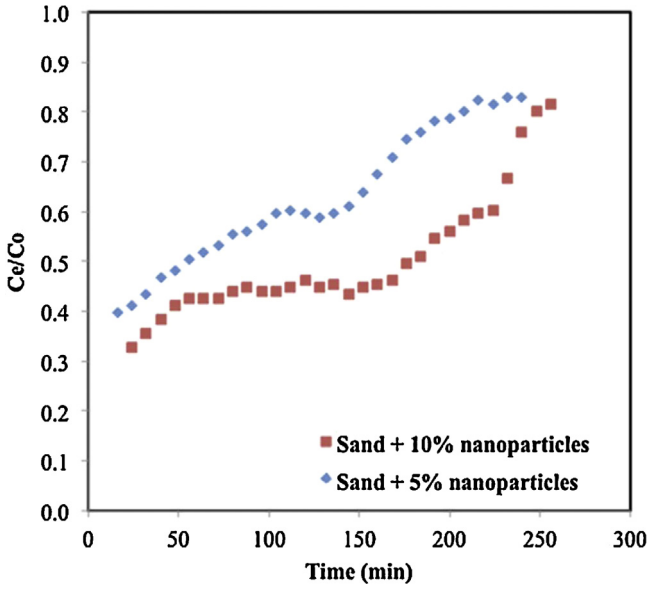

Fig. 5. Breakthrough curves for pollutant adsorption from OMW solution on sand particles with different wt% of γ-Fe_2O_3 nanoparticles at flowrate of 0.03 L/h, pH = 5, T = 298 K and inlet COD concentration of 79,000 mg/L.

As seen in Fig. 6, the first sample obtained at time t = 0 is obviously colorless and more close to the color of pure water. After 30 min, the sample was still colorless, and then after 60, 180 and 240 min it become obvious that the color become pale yellow; but its color density is different from the original control sample. These results are promising since the saturation time, where the ratio C_e/C_i = 1.0, will be long.

One selected sample (i.e., sample obtained after 60 min in the breakthrough curve of 10 wt% nanoparticles) was analyzed for its polyphenols content to estimate their removal efficiency. The initial concentration of polyphenols in the original sample was 7800 mg/L, and after treatment it become 2200 mg/L. This indicates that the polyphenol removal efficiency is approximately 72% after 60 min breakthrough time. Hence, a 100% removal is possible by either increasing the concentration of nanoparticles in the fixed-bed column or by adding another fixed-bed column in series. Accordingly, the treated OMW could be reused in the same olive mill press process to reduce fresh water consumption or safely discharged onto the environment, or used as fertilizer or for irrigation purposes (Komnitsas and Zaharaki, 2012).

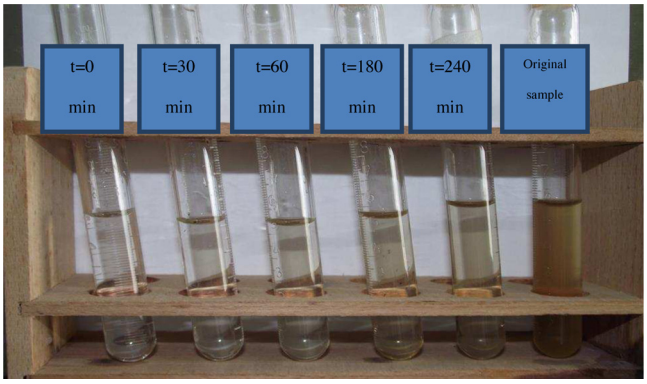

Fig. 6. A photograph of a set of different samples obtained at different times from a fixed bed column of a combination of 10 g of fine sand particles mixed well with 1 g of γ-Fe_2O_3 nanoparticles. The flow rate = 0.03 L/h, T = 298 K, and pH = 5.

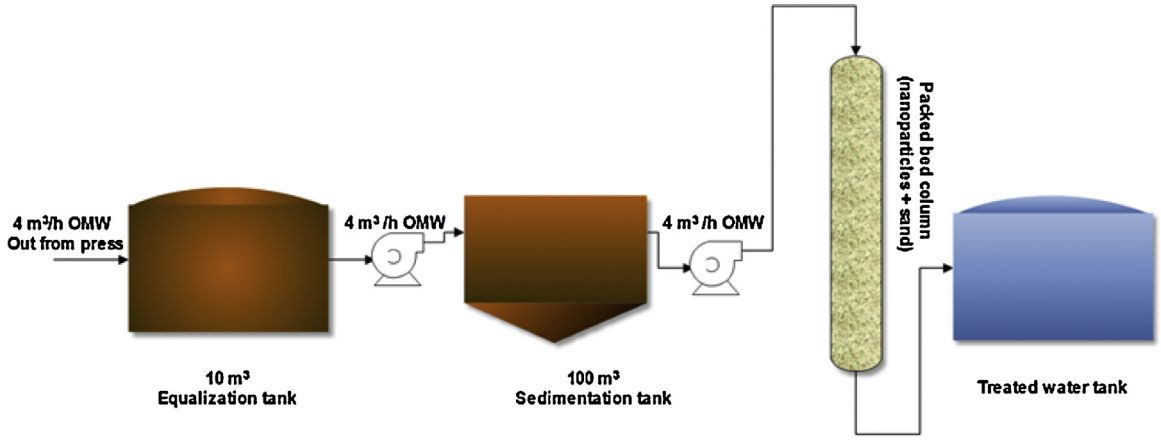

Fig. 7. Block flow diagram of in situ OMW stand-alone treatment plant.

Table 7
Major equipment items and their process description and cost estimation for stand-alone OMW treatment plant.

Element	Descriptions	Capital cost ($)	Annual operating cost ($/year)
Piping system	30 m length and 40 mm nominal diameter high density polyethylene (HDPE).	140	–
Equalization tank	Circular shape carbon steel tank of 3 m diameter and 1.5 m height. The tank is supported by a reinforced concrete base.	893	–
Sedimentation tank	Rectangular tank of 4.1 m height and 25 m^2 cross sectional area. The tank features allow self-cleaning and easily sludge removal. The tank is supported by a reinforced concrete.	9390	–
Nano-sand packed bed	The effluent enters the column by a shower distribter to distribute the flow and prevent chanelling. The first layer is a virgin sand layer with a particle diameter less than 0.1 mm and the total height of the layer is 20 cm. The middle layer consists from the same type of sand mixed with γ-Fe_2O_3 nanoparticles in a percentage of 10% (w/w) (nanoparticles/sand). The total height of the middle layer is 160 cm. The lower layer is a gravel supporter with average particle diameter of 2 cm. The total height of the lower layer is 20 cm. Finally, the bottom of the column is filled with a cotton layer to prevent the escaping of nanoparticles or sand with the treated water. The column is made from carbon steel and is supported by a concrete base.	380	–
Pump A	0.5 hp centrifugal pump to transfer the effluent from the equalization tank to the sdimentation tank.	130	132
Pump B	The size of this pump (4 hp) was selected according to the total headlosses in the piping system and pressure drop inside the fixed bed which was calculated using Ergun equation (Bird et al., 2001).	1000	344
Gate valves	Four (4) 40 mm nominal diameter manual gates valves used to adjust the flowrate.	80	
Sand	Locally available.	134	–
γ-Fe_2O_3 nanoparticles	Locally manufactured.	159	–
Total		12,306	476

4.6. Process description and cost estimation for stand-alone treatment plant

After the successful achievement of the employment of nanoparticle technology in OMW treatment, techno-economical study is carried out for the assessment of the tested results on the performance of typical wastewater treatment systems for a typical olive mill press. As reported in literature, 1–1.8 m^3 of OMW is generated for every ton of olive fruit pressed (El-Gohary et al., 2009). Hence, as the majority of olive presses in Palestine and worldwide working in a capacity of 3 tons of olive per hour, the estimated generation of OMW effluents is approximately 3–5.4 m^3/h. However, these numbers are affected by many factors, such as operating time, type of olive, type of olive presses, etc. Anyhow, 4 m^3/h as effluent flow rate is safe to consider in this study. Fig. 7 shows the typical block flow diagram of the suggested in situ OMW stand-alone treatment plant.

As seen, OMW effluent leaves the olive mill press to enter an equalization tank, which is used to regulate the flow, hold the effluent when the system is shutdown, and adjust the process conditions to meet the treatment requirement (e.g., pH, flow rate, concentration, etc.). Then, the effluent leaves the equalization tank to enter a sedimentation tank for a residence time of 24 h to allow big particles to settle down, according to the experimental results discussed in Section 2.4. Finally, the supernatant is withdrawn and pressurized to enter a fixed-bed column that combines fine sand particles (i.e., less than 0.1 mm) with γ-Fe_2O_3 nanoparticles. Table 7 lists the major equipment required for the stand-alone OMW treatment process plant together with their capital and operating costs. As seen, the capital cost of the entire project is $12,306, this cost is relatively inexpensive comparing with other commercial techniques or conventional treatment stations. Also, the annual operating cost is very low comparing to the amount of water that will be treated and the environmental benefits.

5. Conclusion

In this study, γ-Fe_2O_3 nanoparticles were employed successfully for decolourization, dephenolization and COD removal from synthetic and diluted real olive mill wastewater (OMW). The phenol/COD adsorption rate was fast and equilibrium was achieved within times of less than 10 min for the case of phenol and 30 min for the case of COD in OMW. The adsorption isotherms were also determined and were appropriately described by the BET adsorption model; while the pseudo second-order model appropriately described the adsorption kinetics. In addition to removal of organic pollutants, γ-Fe_2O_3 nanoparticles were able to adsorb other coexisting contaminants to different degrees, such as Fe^{3+}, Cr^{2+}, Cu^{2+}, Ca^{2+}, K^{+}, and Na^{+}. This suggests that the nanoparticles have multi-adsorption sites that can accommodate different types of contaminants, which also enhances multilayer adsorption. Integrating nanoparticle adsorption with fixed bed sand filtration was achieved successfully. The presence of nanoparticles caused a significant decrease in the COD concentration of the effluent at the same time. This is because of the increase in the surface area of adsorbent in the presence of nanoparticles, which provided more active sites for the adsorption. Preliminary process description and cost estimation for stand-alone OMW treatment plant has been demonstrated successfully. The process capital cost was estimated to be $12,306, while the annual operating cost was estimated to be $476/year. This plant is expected to treat a typical flow rate of OMW of 4 m^3/h. Therefore, the plant can be easily integrated with olive mill processes which will favor the economic value of the whole plant, reduce fresh water consumption and enhance water recyclability. Finally, this study confirms that γ-Fe_2O_3 nanoparticles could be employed as an alternative technology for the removal of OMW pollutants. This nanoparticle technology is expected to be cost-effective as nanoparticles could be employed in situ or can be easily incorporated with the conventional treatment technology. Further, this study will provide valuable insight on the effect of nanoparticles toward the treatment and recyclability of olive mill wastewater, which is crucial for the local olive mill industry.

Acknowledgements

The authors thank Mr. N. Dwikat from the Department of Chemistry for his assistance in the UV–vis and AA analysis, the Department of Chemical Engineering for providing the COD kits, and Mrs. Hamees Tbaileh and Mr. Yusef Ratrout for their help in OMW sample characterizations. Special thank to Ms. Nahawand Souqieh from the Palestinian Ministry of Agriculture for her help in conducting the polyphenols tests. The authors would like to thank the Engineer Zuhair Hijjawi Award 2014. Dr. Nassar thanks the Palestinian American Research Center for the 2014/2015 fellowship.

References

Achak, M., Mandi, L., Ouazzani, N., 2009a. Removal of organic pollutants and nutrients from olive mill wastewater by a sand filter. J. Environ. Manage. 90, 2771–2779.

Achak, M., Ouazzani, N., Mandi, L., 2009b. Treatment of modern olive mill effluent by infiltration-percolation on a sand filter. Traitement des margines d'une huilerie moderne par infiltration-percolation sur un filtre à sable 22, 421–433.

Achak, M., Ouazzani, N., Yaacoubi, A., Mandi, L., 2008. Modern olive mill effluent characterization and their treatment by coagulation–flocculation using lime and aluminium sulphate. Caractérisation des margines issues d'une huilerie moderne et essais de leur traitement par coagulation-floculation par la chaux et le sulfate d'aluminium 21, 53–67.

Akdemir, E.O., Ozer, A., 2009. Investigation of two ultrafiltration membranes for treatment of olive oil mill wastewater. Desalination 249, 660–666.

ASTM, 1995. Standard Test Methods for Chemical Oxygen Demand (Dichromate Oxygen Demand) of Water. American Society for Testing and Materials, Philadelphia, PA.

Azbar, N., Keskin, T., Catalkaya, E.C., 2008a. Improvement in anaerobic degradation of olive mill effluent (OME) by chemical pretreatment using batch systems. Biochem. Eng. J. 38, 379–383.

Azbar, N., Keskin, T., Yuruyen, A., 2008b. Enhancement of biogas production from olive mill effluent (OME) by co-digestion. Biomass Bioenergy 32, 1195–1201.

Balistrieri, L.S., Murray, J.W., 1981. The surface chemistry of goethite (aFeOOH) in major ion seawater. Am. J. Sci., 788–806.

Ben Sassi, A., Ouazzani, N., Walker, G.M., Ibnsouda, S., El Mzibri, M., Boussaid, A., 2008. Detoxification of olive mill wastewaters by Moroccan yeast isolates. Biodegradation 19, 337–346.

Bird, R.B., Stewart, W.E., Lightfoot, E.N., 2001. Transport Phenomena. Wiley, New York.

Boubaker, F., Ridha, B.C., 2008. Modelling of the mesophilic anaerobic co-digestion of olive mill wastewater with olive mill solid waste using anaerobic digestion model No. 1 (ADM1). Bioresour. Technol. 99, 6565–6577.

Boukhoubza, F., Ait Boughrous, A., Yacoubi-Khebiza, M., Jail, A., Hassani, L., Loukili Idrissi, L., Nejmeddine, A., 2008. Impact of olive oil wastewater on the physicochemical and biological quality of groundwater in the Haouz plain, south of Marrakesh (Morocco). Impact des effluents des huileries d'olive sur la qualité physico-chimique et biologique des eaux souterraines dans la plaine du Haouz au sud de Marrakech (Maroc) 29, 959–974.

Box, J.D., 1983. Investigation of the Folin–Ciocalteau phenol reagent for the determination of poly phenolic substances in natural waters. Water Res., 511–525.

Brunetti, G., Senesi, N., Plaza, C., 2007. Effects of amendment with treated and untreated olive oil mill wastewaters on soil properties, soil humic substances and wheat yield. Geoderma 138, 144–152.

Chedeville, O., Debacq, M., Porte, C., 2009. Removal of phenolic compounds present in olive mill wastewaters by ozonation. Desalination 249, 865–869.

Choy, K.K.H., Barford, J.P., McKay, G., 2005. Production of activated carbon from bamboo scaffolding waste—process design, evaluation and sensitivity analysis. Chem. Eng. J. 109, 147–165.

Clifford, A.B., Luis, S., 1979. Hydrophobic and coulombic interactions in the micellar binding of phenols and phenoxide ions. J. Phys. Chem., 680–683.

Coskun, T., Debik, E., Demir, N.M., 2010. Treatment of Olive Mill Wastewaters by Nanofiltration and Reverse Osmosis Membranes. Elsevier, pp. 65–70.

Crittenden, J.C., 2005. Water Treatment: Principles and Design. Wiley, Hoboken, NJ.

Dhaouadi, H., Marrot, B., 2008. Olive mill wastewater treatment in a membrane bioreactor: process feasibility and performances. Chem. Eng. J. 145, 225–231.

Ebadi, A., Soltan Mohammadzadeh, J., Khudiev, A., 2009. What is the correct form of BET isotherm for modeling liquid phase adsorption? Adsorption 15, 65–73.

El Saliby, I., Shon, H., Kandasamy, J., Vigneswaran, S., 2009. Nanotechnology for water and wastewater treatment: in brief. In: Vigneswaran, S.V. (Ed.), Water and Wastewater Treatment Technologies. Encyclopedia of Life Support Systems (EOLSS).

El-Gohary, F.A., Badawy, M.I., El-Khateeb, M.A., El-Kalliny, A.S., 2009. Integrated treatment of olive mill wastewater (OMW) by the combination of Fenton's reaction and anaerobic treatment. J. Hazard. Mater. 162, 1536–1541.

Eroğlu, E., Eroğlu, I., Gündüz, U., Yücel, M., 2008. Effect of clay pretreatment on photofermentative hydrogen production from olive mill wastewater. Bioresour. Technol. 99, 6799–6808.

Franco, C.A., Cortés, F.B., Nassar, N.N., 2014a. Adsorptive removal of oil spill from oil-in-fresh water emulsions by hydrophobic alumina nanoparticles functionalized with petroleum vacuum residue. J. Colloid Interface Sci. 425, 168–177.

Franco, C.A., Nassar, N.N., Cortés, F.B., 2014b. Removal of oil from oil-in-saltwater emulsions by adsorption onto nano-alumina functionalized with petroleum vacuum residue. J. Colloid Interface Sci. 433, 58–67.

Garcia, G., Jimenez, P.R., Venceslada, J.L., Martin, A., Santos, M.A., Gomez, E., 2000. Removal of phenol compounds from olive oil mill wastewater using *Phanerochaete chrysosporium*, *Aspergillus niger*, *Aspergillus terreus* and *Geotrichum candidum*. Process Biochem. 35, 751–758 (Elsevier Science Ltd.).

Gomec, C.Y., Erdim, E., Turan, I., Aydin, A.F., Ozturk, I., 2007. Advanced oxidation treatment of physico-chemically pre-treated olive mill industry effluent. J. Environ. Sci. Health B 42, 741–747.

Hanafi, F., Sadif, N., Assobhei, O., Mountadar, M., 2009. Olive oil mill wastewater treatment by means of electrocoaculation with punts aluminium electrodes. Traitement des margines par électrocoagulation avec des électrodes plates en aluminium 22, 473–485.

Hanifi, S., El Hadrami, I., 2009. Olive mill wastewaters: diversity of the fatal product in olive oil industry and its valorisation as agronomical amendment of poor soils: a review. J. Agronomy 8, 1–13.

Ho, Y.S., 2004. Citation review of Lagergren kinetic rate equation on adsorption. Scientometrics, 171–177.

Ho, Y.S., McKay, G., 1998. A comparison of chemisorption kinetic models applied to pollutant removal on various sorbents. Process Saf. Environ. Protect., 332–340.

Ipsilantis, I., Karpouzas, D.G., Papadopoulou, K.K., Ehaliotis, C., 2009. Effects of soil application of olive mill wastewaters on the structure and function of the community of arbuscular mycorrhizal fungi. Soil Biol. Biochem. 41, 2466–2476.

Jarboui, R., Sellami, F., Kharroubi, A., Gharsallah, N., Ammar, E., 2008. Olive mill wastewater stabilization in open-air ponds: impact on clay-sandy soil. Bioresour. Technol. 99, 7699–7708.

Kallel, M., Belaid, C., Boussahel, R., Ksibi, M., Montiel, A., Elleuch, B., 2009. Olive mill wastewater degradation by Fenton oxidation with zero-valent iron and hydrogen peroxide. J. Hazard. Mater. 163, 550–554.

Kaur, A., Gupta, U., 2009. A review on applications of nanoparticles for the preconcentration of environmental pollutants. J. Mater. Chem. 19, 8279–8289.

Komnitsas, K., Zaharaki, D., 2012. Pre-treatment of olive mill wastewaters at laboratory and mill scale and subsequent use in agriculture: legislative framework and proposed soil quality indicators. Resour. Conserv. Recycl. 69, 82–89.
Lucas, M.S., Peres, J.A., 2009. Removal of COD from olive mill wastewater by Fenton's reagent: kinetic study. J. Hazard. Mater. 168, 1253–1259.
Montgomery, D.C., Runger, G.C., 2006. Applied Statistics and Probability for Engineers. John Wily & Sons Inc., New York.
Narayan, R., 2010. Use of nanomaterials in water purification. Mater. Today 13, 44–46.
Nassar, M.A., 2007. Olive mill wastewater treatment methods. In: International Arab Conference for Oils and Food Fats, 2007 Damascus. IACOFF, pp. 9–11.
Nassar, N.N., 2010a. Kinetics, mechanistic, equilibrium, and thermodynamic studies on the adsorption of acid red dye from wastewater by γ-Fe_2O_3 nanoadsorbents. Sep. Sci. Technol. 45, 1092–1103.
Nassar, N.N., 2010b. Rapid removal and recovery of Pb(II) from wastewater by magnetic nanoadsorbents. J. Hazard. Mater. 184, 538–546.
Nassar, N.N., 2012a. Iron oxide nanoadsorbents for removal of various pollutants from wastewater: an overview. In: Bhatnagar, A. (Ed.), Application of Adsorbents for Water Pollution Control. Bentham Science Publishers.
Nassar, N.N., 2012b. Kinetics, equilibrium and thermodynamic studies on the adsorptive removal of nickel, cadmium and cobalt from wastewater by superparamagnetic iron oxide nanoadsorbents. Can. J. Chem. Eng., 1231–1238.
Nassar, N.N., 2013. The application of nanoparticles for wastewater remediation. In: Bruggen, B.V.D. (Ed.), Applications of Nanomaterials for Water Quality. Future Science, London, UK.
Nassar, N.N., Ringsred, A., 2012. Rapid adsorption of methylene blue from aqueous solutions by goethite nanoadsorbents. Environ. Eng. Sci., 790–797.
Ochando-Pulido, J.M., Hodaifa, G., Víctor-Ortega, M.D., Martínez-Ferez, A., 2013. A novel photocatalyst with ferromagnetic core used for the treatment of olive oil mill effluents from two-phase production process. ScientificWorldJournal, 2013.
Paraskeva, C.A., Papadakis, V.G., Tsarouchi, E., Kanellopoulou, D.G., Koutsoukos, P.G., 2007. Membrane processing for olive mill wastewater fractionation. Desalination 213, 218–229.
Ruzmanova, I., Stoller, M., Chianese, A., 2013. Photocatalytic treatment of olive mill waste water by magnetic core titanium dioxide nanoparticles. Chem. Eng., 32.
Savage, N., Diallo, M.S., 2005. Nanomaterials and water purification: opportunities and challenges. J. Nanopart. Res. 7, 331–342.
Shaheen, H., Karim, R.A., 2007. Management of Olive–Mills Wastewater in Palestine. An-Najah Sci. J., 63–83.
Sing, K.S.W., Everett, D.H., Haul, R., Moscou, L., Pierotti, R.A., Rouquerol, J., Siemieniewska, T., 1982. Reporting physisorption data for gas/solid systems with special reference to the determination of surface area and porosity. Pure Appl. Chem. 54, 2201.
Teller, E., Brunauer, S., Emmett, H., 1938. Adsorption of gases in multimolecular layers. J. Am. Chem. Soc., 309.
Tratnyek, P.G., Johnson, R.L., 2006. Nanotechnologies for environmental cleanup. Nano Today 1, 44–48.
Ugurlu, M., Kula, I., 2007. Decolourization and removal of some organic compounds from olivemill wastewater by advanced oxidation processes and lime treatment. Environ. Sci. Pollut. Res., 319–325.
Wang, J., Huang, C.P., Allen, H.E., Cha, D.K., Kim, D.-W., 1998. Adsorption characteristics of dye onto sludge particulates. J. Colloid Interface Sci. 208, 518–528.
Weng, C.-H., Pan, Y.-F., 2006. Adsorption characteristics of methylene blue from aqueous solution by sludge ash. Colloids Surf. A: Physicochem. Eng. Aspects 274, 154–162.
Weng, C.-H., Pan, Y.-F., 2007. Adsorption of a cationic dye (methylene blue) onto spent activated clay. J. Hazard. Mater. 144, 355–362.
Xu, P., Zeng, G.M., Huang, D.L., Feng, C.L., Hu, S., Zhao, M.H., Lai, C., Wei, Z., Huang, C., Xie, G.X., Liu, Z.F., 2012. Use of iron oxide nanomaterials in wastewater treatment: a review. Sci. Total Environ. 424, 1–10.
Zorpas, A.A., Costa, C.N., 2010. Combination of Fenton oxidation and composting for the treatment of the olive solid residue and the olive mile wastewater from the olive oil industry in Cyprus. Bioresour. Technol. 101, 7984–7987.